High efficiency of nitric acid controls in alleviating particulate nitrate in livestock and urban areas in South Korea

Haeri Kim,[a] Junsu Park,[a] Seunggi Kim,[a] Komal Narayan Pawar[a] and Mijung Song*[ab]

a. Department of Environment and Energy, Jeonbuk National University, Jeonju 54896, Korea.
b. Department of Earth and Environmental Sciences, Jeonbuk National University, Jeonju 54896, Korea.

S1. Comparison of measurements and modeling

Fig. S2 illustrates the scatter plots of the observed versus estimated total HNO_3 (TN) in the livestock area during the entire measurement period. A high correlation (R^2 = 0.88, slope = 0.97) was observed between the estimated and observed TN concentrations (Fig. S2). Moreover, the performance of ISORROPIA-II was verified by comparing the predicted and observed concentrations of the major secondary inorganic aerosol (SIA) species, NO_3^-, SO_4^{2-}, and NH_4^+. As shown in Fig. S3, the measured NO_3^- and NH_4^+ concentrations at the livestock site were found to be slightly lower than the predicted concentrations, which might be due to the partial evaporation of semi-volatile inorganic aerosol components on the filters during study periods.[1, 2] However, good correlations (R^2 = 0.81–0.99, slopes = 0.88–0.98 for the livestock area, and R^2 = 0.95–0.99, slopes = 0.90–1.00 for the urban area) were observed between the predicted results and observations, indicating the good performance of the ISORROPIA-II model for reliable prediction of SIA species.

Supplementary Figure

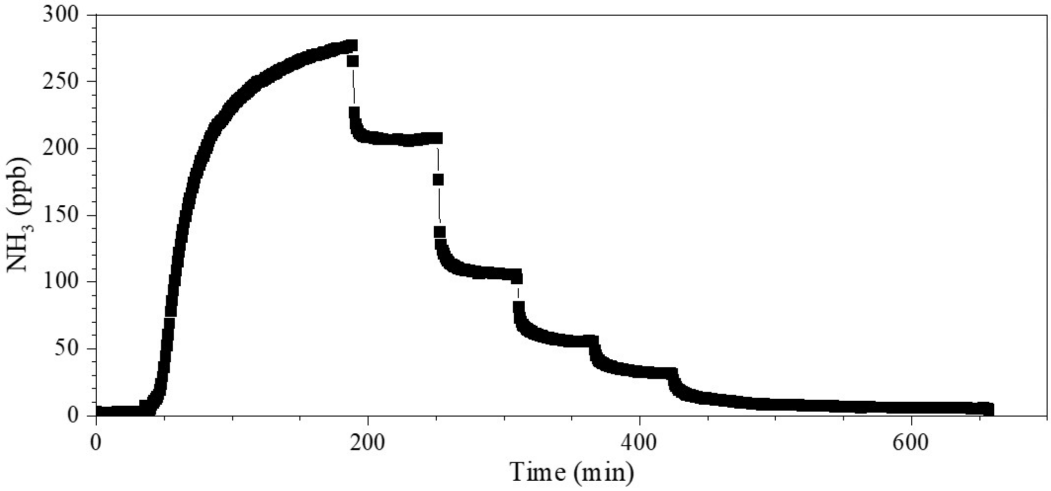

Fig. S1 Calibration of the NH_3 instrument using diluted standard NH_3 and N_2 gas.

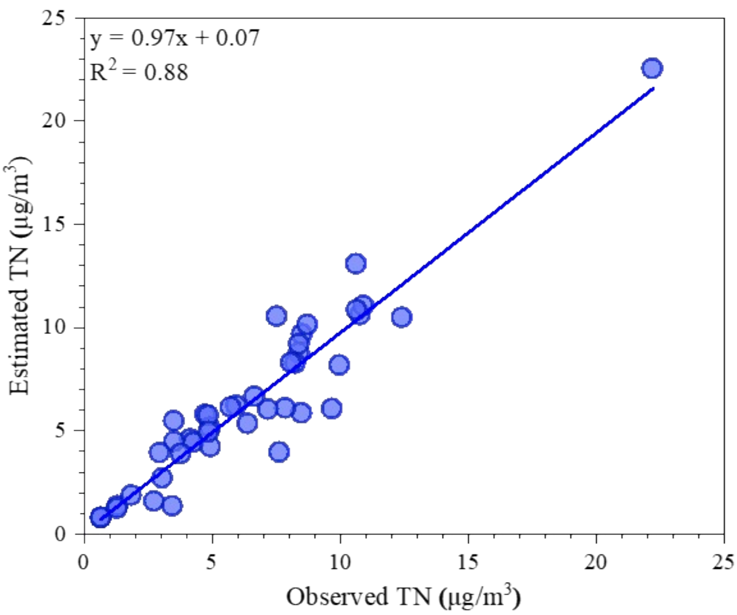

Fig. S2 Comparison of observed and estimated data of total nitrate (TN) for the livestock area during measurement periods.

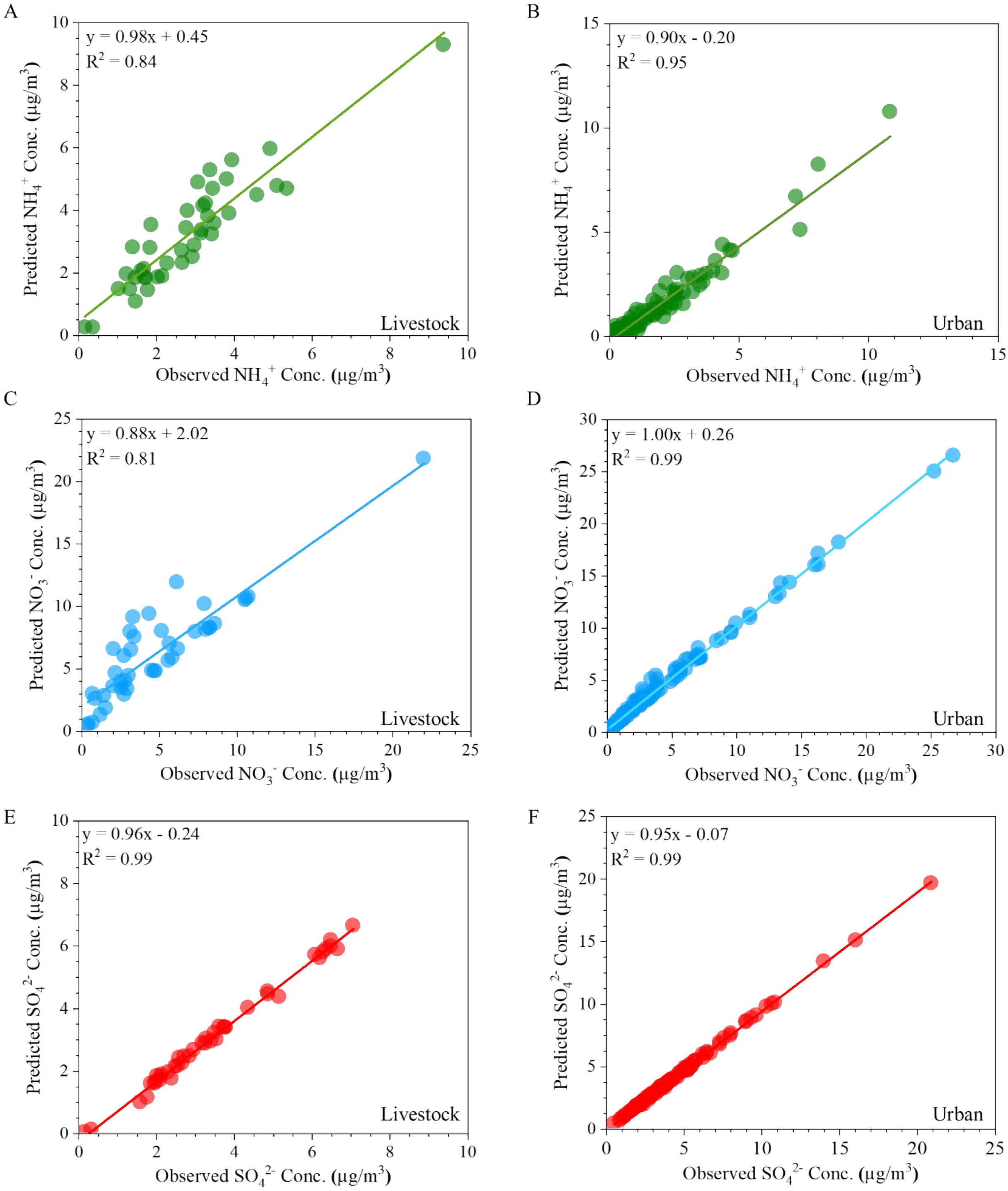

Fig. S3 Comparison of observed and predicted values of (A and B) NH_4^+, (C and D) NO_3^- and (E and F) SO_4^{2-} during study periods in livestock, and urban areas.

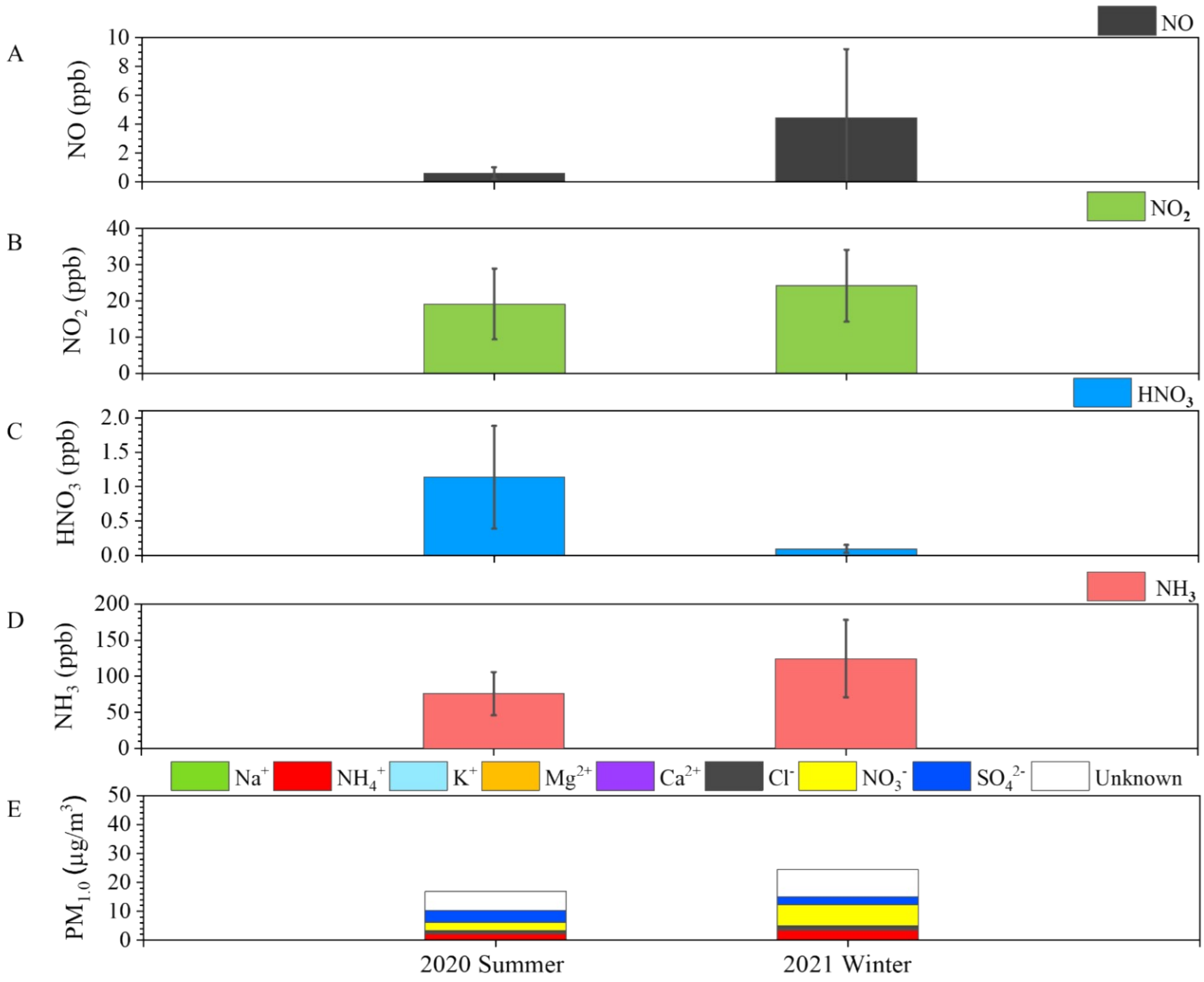

Fig. S4 Average daily concentrations of (A) NO, (B) NO_2 (C) HNO_3, (D) NH_3 and (E) water-soluble ions in $PM_{1.0}$ measured in the livestock area during the summer and winter.

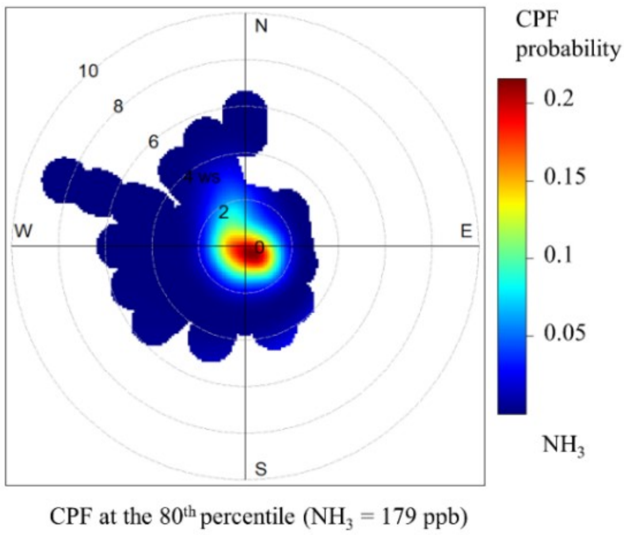

Fig. S5 Conditional probability function (CPF) result at the 80th percentile for atmospheric NH_3 during pollution days in the livestock area.

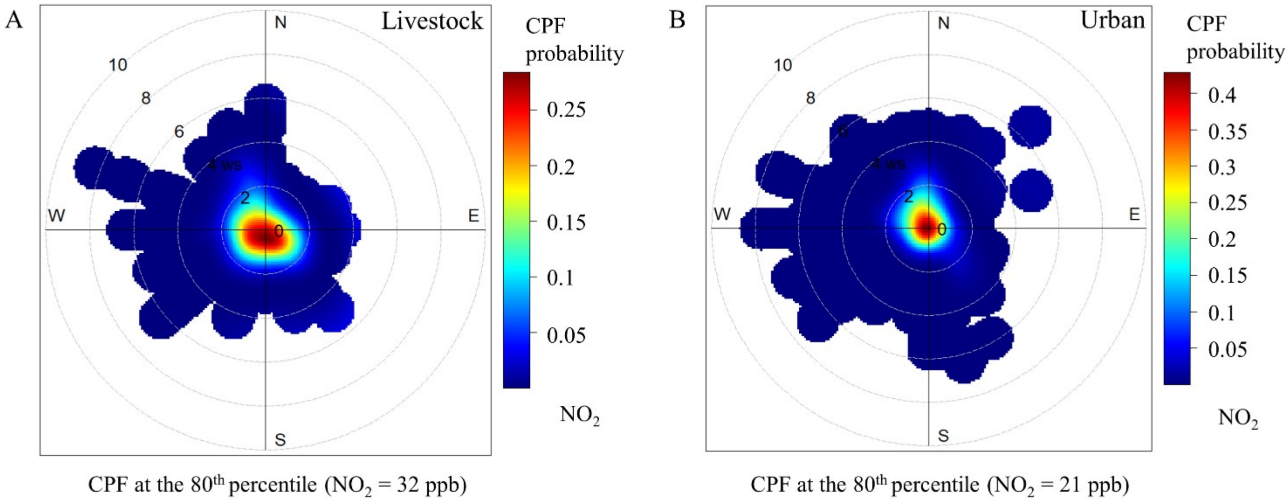

Fig. S6 Conditional probability function (CPF) result at the 80th percentile for the atmospheric NO_2 in (A) livestock and (B) urban areas[3] during measurement periods.

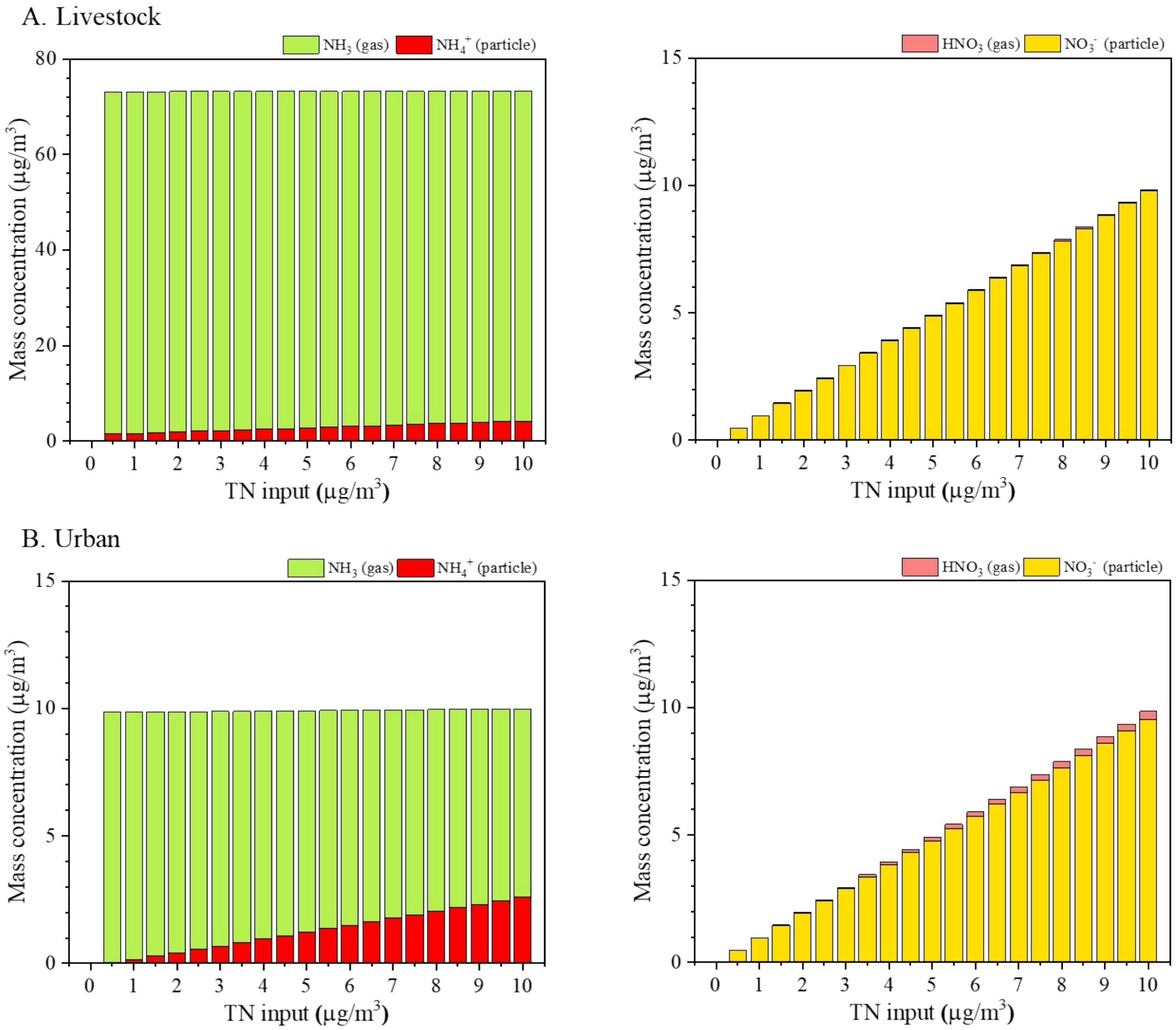

Fig. S7 Thermodynamic model simulations using ISORROPIA-II for gas-particle partitioning of HNO_3 and NH_3 varied by the total nitrate (TN) concentrations in (A) livestock and (B) urban areas.

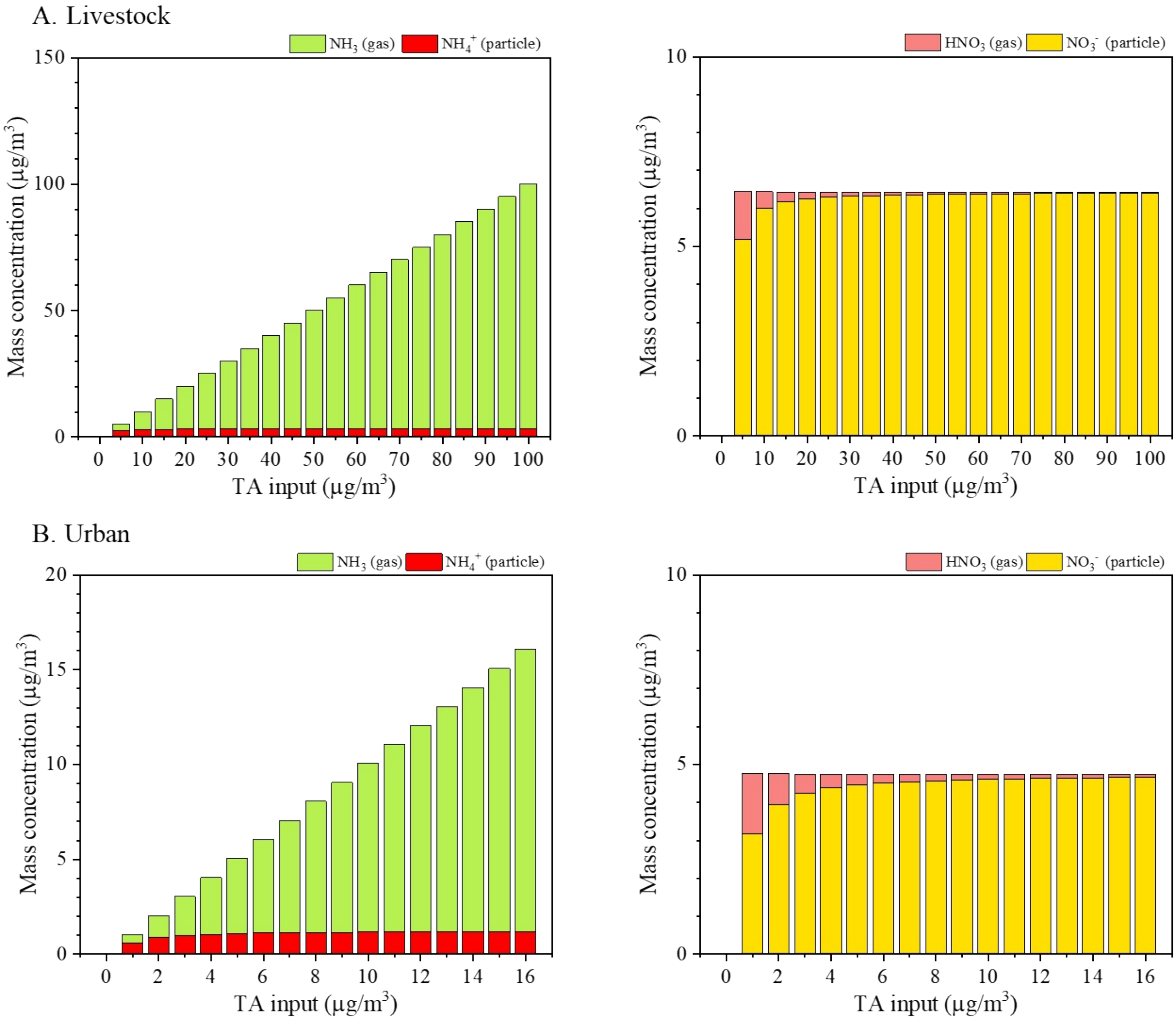

Fig. S8 Thermodynamic model simulations using ISORROPIA-II for gas-particle partitioning of HNO_3 and NH_3 varied by the total ammonia (TA) concentrations in (A) livestock and (B) urban areas.

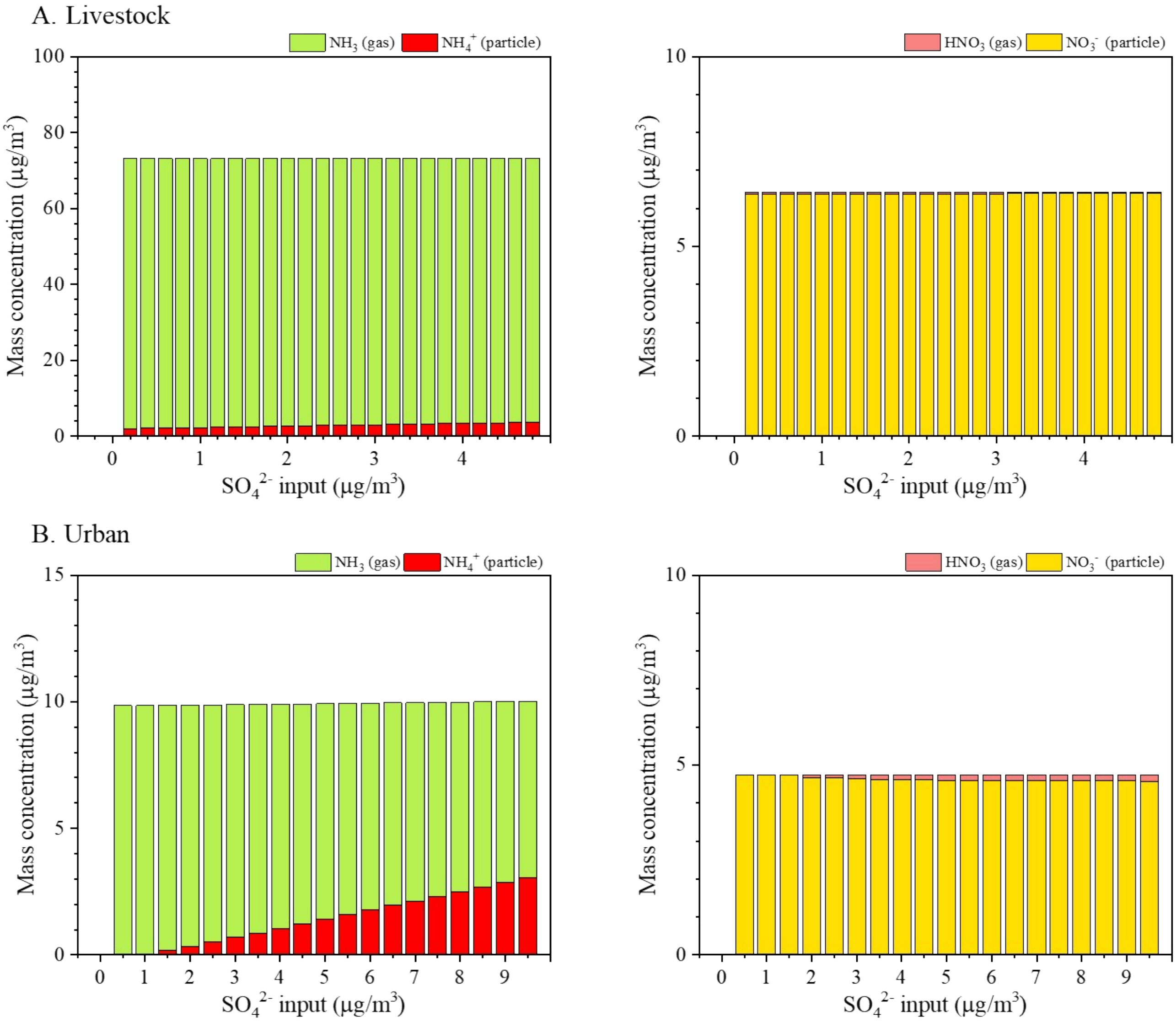

Fig. S9 Thermodynamic model simulations using ISORROPIA-II for gas-particle partitioning of HNO_3 and NH_3 varied by the SO_4^{2-} concentrations in (A) livestock and (B) urban areas.

Supplementary Table

Table. S1 The average seasonal concentration of gaseous species, chemical compositions and meteorological parameters with the standard deviation in livestock and urban areas during entire days. Jeonju data is from Park et al., (2021).

	Jeonju (urban)[3]	Gimje (Livestock)		
Species	**Entire**	**Entire**	**Summer**	**Winter**
Aerosol species (μg /m^3)				
$PM_{1.0}$	-	20.1 ± 8.8	16.9 ± 7.5	24.4 ± 8.4
$PM_{2.5}$	24.0 ± 12.8	-	-	-
Na^+	2.2 ± 0.9	0.08 ± 0.06	0.08 ± 0.06	0.08 ± 0.07
NH_4^+	1.6 ± 1.8	2.8 ± 1.6	2.3 ± 1.2	3.5 ± 1.8
K^+	0.3 ± 0.3	0.2 ± 0.1	0.2 ± 0.1	0.2 ± 0.1
Mg^{2+}	0.02 ± 0.01	0.02 ± 0.01	0.02 ± 0.01	0.02 ± 0.01
Ca^{2+}	0.08 ± 0.05	0.1 ± 0.05	0.1 ± 0.04	0.1 ± 0.06
Cl^-	0.5 ± 0.6	0.9 ± 0.6	0.7 ± 0.4	1.1 ± 0.7
NO_3^-	4.4 ± 4.9	4.8 ± 3.9	2.9 ± 1.8	7.3 ± 4.5
SO_4^{2-}	4.3 ± 3.1	3.5 ± 1.8	4.1 ± 2.0	2.7 ± 0.9
Gaseous pollutants (ppb)				
NH_3	10.5 ± 4.8	96.9 ± 48.1	76.0 ± 29.8	124.6 ± 53.6
HNO_3	0.2 ± 0.2*	0.7 ± 0.7	1.1 ± 0.7	0.1 ± 0.1
NO_2	15.5 ± 5.8	21.3 ± 10.2	19.2 ± 9.8	24.2 ± 9.9
TA	13.8 ± 3.9	101.4 ± 36.8	79.2 ± 21.5	128.8 ± 39.8
TN	1.7 ± 5.0*	2.4 ± 3.9	2.2 ± 3.2	2.7 ± 4.5
Meteorological parameters				
Temperature (℃)	13.0 ± 7.5	15.1 ± 9.8	23.2 ± 1.8	4.4 ± 4.2
Relative humidity (%)	64.4 ± 11.5	74.7 ± 11.3	79.4 ± 7.1	68.5 ± 12.8

*Estimation based on an equation from Seo et al., 2020

Reference

1. D. H. Huy, T. T. Hien and N. Takenaka, Comparative study on water-soluble inorganic ions in $PM_{2.5}$ from two distinct climate regions and air quality, *Journal of Environmental Sciences*, 2020, **88**, 349-360. DOI: 10.1016/j.jes.2019.09.010.
2. V. Karydis, A. Tsimpidi, A. Pozzer, M. Astitha and J. Lelieveld, Effects of mineral dust on global atmospheric nitrate concentrations, *Atmospheric Chemistry and Physics*, 2016, **16**, 1491-1509. DOI: 10.5194/acp-16-1491-2016.
3. J. Park, E. Kim, S. Oh, H. Kim, S. Kim, Y. P. Kim and M. Song, Contributions of Ammonia to High Concentrations of $PM_{2.5}$ in an Urban Area, *Atmosphere*, 2021, **12**, 1676. DOI: 10.3390/atmos12121676.
4. J. Seo, Y. B. Lim, D. Youn, J. Y. Kim and H. C. Jin, Synergistic enhancement of urban haze by nitrate uptake into transported hygroscopic particles in the Asian continental outflow, *Atmospheric Chemistry and Physics*, 2020, **20**, 7575-7594. DOI: 10.5194/acp-20-7575-2020.